

Showcasing collaborative research from Prof. Dr Haibo Zhang (Wuhan University, China) and Dr Khaleel I. Assaf (Jacobs University Bremen, Germany).

The chaotropic effect as an orthogonal assembly motif for multi-responsive dodecaborate-cucurbituril supramolecular networks

The chaotropic effect between dodecaborate anions and cucurbiturils was introduced as a novel assembly motif. Based on the marriage of the chaotropic and hydrophobic effects, supramolecular networks with multi-responsive behaviors can be built totally through noncovalent interactions.

As featured in:



See Khaleel I. Assaf,  
Haibo Zhang *et al.*,  
*Chem. Commun.*, 2018, 54, 2098.

Cite this: *Chem. Commun.*, 2018, 54, 2098Received 19th October 2017,  
Accepted 3rd January 2018

DOI: 10.1039/c7cc08078f

rsc.li/chemcomm

# The chaotropic effect as an orthogonal assembly motif for multi-responsive dodecaborate-cucurbituril supramolecular networks†

Wenjing Wang,<sup>a</sup> Xiaoqiang Wang,<sup>a</sup> Jin Cao,<sup>b</sup> Jun Liu,<sup>c</sup> Bin Qi,<sup>a</sup> Xiaohai Zhou,<sup>a</sup> Shuai Zhang,<sup>d</sup> Detlef Gabel,<sup>d</sup> Werner M. Nau,<sup>d</sup> Khaleel I. Assaf<sup>ib</sup>\*<sup>d</sup> and Haibo Zhang<sup>ib</sup>\*<sup>a</sup>

In aqueous solution, host–guest complexation is frequently driven by the hydrophobic effect, which also constitutes a popular approach in the design of supramolecular assemblies. Herein, we report an orthogonal assembly motif, the chaotropic effect, which exploits the tendency of chaotropic anions to associate with hydrophobic surfaces.

Supramolecular chemistry provides a tool for designing novel functional materials. For example, supramolecular polymers, combining the outstanding properties of traditional polymers and the controllable features of supramolecular systems, show very interesting and versatile properties due to their dynamic and designable nature.<sup>1</sup> They have potential applications, among others, for cargo delivery, micropollutant removal, biomaterial scaffolds, and materials science.<sup>2</sup> For supramolecular materials in water, the building blocks are often low-molecular weight monomeric units brought together by the hydrophobic effect, assisted and directed by additional noncovalent interactions, such as hydrogen bonding, electrostatic interactions or metal–ligand coordination.<sup>3</sup> Macrocyclic host molecules have become particularly attractive in the formation of supramolecular networks, because they allow the site-specific formation of both exclusion and inclusion complexes.<sup>4</sup>

Dodecaborate clusters are inorganic anions, which have an icosahedral structure with a permanent double negative charge.<sup>5</sup> As efficient <sup>10</sup>B-enriched reagents, they have numerous applications in medicinal chemistry and materials science, especially in

boron neutron capture therapy.<sup>6</sup> Recently, a high propensity for inclusion complex formation of dodecaborate clusters with large cyclodextrins (CDs) has been observed in aqueous solution.<sup>7</sup> The driving force, modulated by dispersion interactions, was attributed to the chaotropic effect, which describes an intrinsic affinity of water-structure breaking (chaotropic) anions to hydrophobic surfaces.<sup>7a,8</sup> The new noncovalent binding motif, which is orthogonal to the hydrophobic effect chemically and thermodynamically,<sup>7a,9</sup> can be extended to the outer surface of cucurbit[*n*]urils (CB*n*, *n* = 5–8), see Fig. 1. CB*n*, a series of pumpkin-shaped glycoluril oligomers, are water-soluble macrocycles with unique recognition properties.<sup>10</sup> They are capable of encapsulating a wide range of organic guest molecules in their hydrophobic cavities.<sup>11</sup> Recently, CB*n* have also been used for constructing supramolecular assemblies and engineering functional materials.<sup>12</sup>

In this work, we introduce, for the first time, the chaotropic effect as a new assembly motif, which exploits the tendency of dodecaborate cluster anions, as superchaotropic anions, to bind to the hydrophobic exterior of CB*n* macrocycles. Complex formation between B<sub>12</sub>H<sub>12</sub><sup>2-</sup> and CB7 was established using <sup>1</sup>H NMR

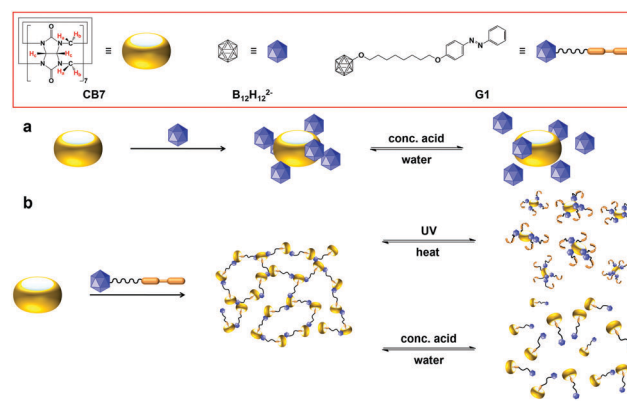


Fig. 1 (a) The self-assembly of CB7 and B<sub>12</sub>H<sub>12</sub><sup>2-</sup> in aqueous solution. (b) Multi-responsive assembly formed between CB7 and G1 in aqueous solution.

<sup>a</sup> College of Chemistry and Molecular Sciences, Wuhan University, Wuhan 430072, China. E-mail: haibo Zhang 1980@gmail.com

<sup>b</sup> Hubei Gedian Humanwell Pharmaceutical Excipients Co., Ltd, Gedian 436070, China

<sup>c</sup> Hunan University of Arts and Science, Changde 415000, China

<sup>d</sup> Department of Life Sciences and Chemistry, Jacobs University Bremen, Campus Ring 1, 28759 Bremen, Germany. E-mail: k.assaf@jacobs-university.de

† Electronic supplementary information (ESI) available: Synthetic details, characterization, binding studies, crystallographic studies and morphological studies. CCDC 1574822, 1574912 and 1574823. For ESI and crystallographic data in CIF or other electronic format see DOI: 10.1039/c7cc08078f



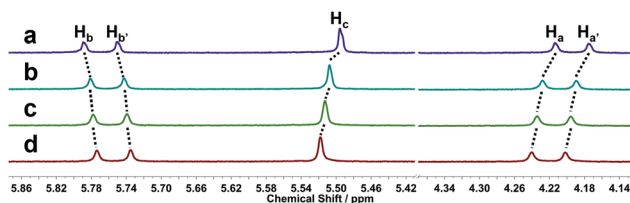


Fig. 2  $^1\text{H}$  NMR spectra of the complex of CB7/ $\text{B}_{12}\text{H}_{12}^{2-}$  (400 MHz,  $\text{D}_2\text{O}$ , 25  $^\circ\text{C}$ ). The concentration of CB7 was kept fixed as 0.4 mM and the concentration of  $\text{Na}_2\text{B}_{12}\text{H}_{12}$  was varied: (a) 0 mM, (b) 0.4 mM, (c) 0.8 mM, and (d) 4.0 mM. Partial aggregation was observed above 0.1 mM. The HOD peak between 4.37 and 5.41 ppm was removed for clarity.

spectroscopy (Fig. 2). In the  $^1\text{H}$  NMR spectra, the B–H protons are not informative, due to the extreme broadness of the B–H resonance (from  $-0.5$  to  $+2.0$  ppm).<sup>7</sup> Instead, we followed the complexation-induced chemical shift of the CB $n$  protons. Sizable shifts of all protons ( $\text{H}_a$ ,  $\text{H}_b$  and  $\text{H}_c$ , see Fig. 1, top left) were observed, in particular upfield shifts of  $\text{H}_a$  and  $\text{H}_c$ , which are co-equatorial and equatorial, respectively, and a downfield shift of  $\text{H}_b$ , positioned co-axially (Fig. 2); this signalled the formation of an exclusion complex, because the CB protons are generally barely affected by the formation of the inclusion complex. Job plot analysis (Fig. S1, ESI<sup>†</sup>) indicated higher-order complexation stoichiometries, while the analysis of the ITC data (Fig. S2, ESI<sup>†</sup>) indicated that the data could be fitted, for example, with a 1:6 binding model and the extracted apparent binding constants were  $10^4$ – $10^5$   $\text{M}^{-1}$ . Aggregate formation at low millimolar concentration (see below) provided visible evidence of the affinity, but prevented an accurate determination of the complexation thermodynamics.

To verify the formation of exclusion complexes between dodecaborate anions and CB $n$ , we screened various dodecaborate clusters ( $\text{B}_{12}\text{Cl}_{11}\text{OH}^{2-}$ ,  $\text{B}_{12}\text{Cl}_{12}^{2-}$  and  $\text{B}_{12}\text{H}_{12}^{2-}$ ) with CB7 and CB6 for single-crystal formation. The XRD structure of the complex between CB7 and  $\text{B}_{12}\text{H}_{11}\text{OH}^{2-}$  shows that each CB7 unit interacts with eight  $\text{B}_{12}\text{H}_{11}\text{OH}^{2-}$  clusters, four above and four below the equator with non-centrosymmetrical distribution (Fig. 3). Two clusters at the same layer are adjacent and connected by a hydrogen bond between the hydroxyl groups (a B–O–H $\cdots$ (O–H)–B motif with a

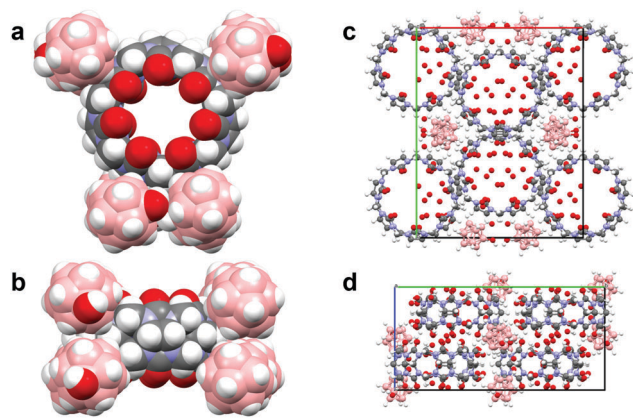


Fig. 3 Views of the CB7/ $\text{B}_{12}\text{H}_{11}\text{OH}^{2-}$  complex XRD structure. The CB7 component has crystallographically-imposed twofold symmetry and that the  $\text{B}_{12}\text{H}_{11}\text{OH}^{2-}$  component is in a general position.

$\text{O}\cdots\text{O}$  bond distance of 2.35 Å). The crystal packing further revealed short contacts between the partially negatively charged hydrogens on the clusters and the carbonyl carbons of CB7 ( $\text{H}\cdots\text{C}=\text{O}$ : 2.5–2.6 Å). A database search (Cambridge Crystallographic Data Centre) to identify the abundance and occurrence of similar intermolecular interactions ( $\text{H}\cdots\text{C}=\text{O}$ ) revealed only three examples (codes: EZIHAX, PERXEP, and WICHEV), all of which involve carborane derivatives. Another unconventional interaction was observed in the crystal structure, in which the partially negative hydrogen atoms on the cluster interact with the hydrogen atoms on the exterior of CB7 ( $\text{H}\cdots\text{H}$  approximately 2.25–2.58 Å). We also obtained single crystals of the complex between CB7 and  $\text{B}_{12}\text{Cl}_{12}^{2-}$  (Fig. S3, ESI<sup>†</sup>), and single crystals of the complex between CB6 and  $\text{B}_{12}\text{H}_{12}^{2-}$  (Fig. S4, ESI<sup>†</sup>). All XRD structures proved the formation of exclusion complexes between dodecaborate clusters and CB $n$ , and thereby confirmed the observations in aqueous solution by  $^1\text{H}$  NMR spectroscopy. Dodecaborate clusters are chaotropic dianions,<sup>7a</sup> they are hydrophilic and their sodium salts are highly water soluble. The general tendency of chaotropic anions to associate with hydrophobic surfaces in aqueous solution has been recently established for cyclodextrins<sup>7a</sup> and referred to as the chaotropic effect, complementing the hydrophobic effect which brings together two hydrophobic partners. This accounts also for the tendency of dodecaborate clusters to associate with CB $n$  macrocycles, although in this case exclusion complexes rather than inclusion complexes are formed. The desolvation of chaotropic anions leads to the restoration of the hydrogen bonding network. This is an enthalpically favorable and entropically penalized process,<sup>7a</sup> which allows these anions to associate with hydrophobic concave and convex surfaces with overall negative free energies.

The XRD structures of the exclusion complexes reveal additional details, which can be rationalized from the electrostatic potential (ESP) maps of the dodecaborate anions and CB $n$  macrocycles (Fig. 4). For the dodecaborate, the double negative charge is evenly dispersed over the cluster sphere. On the other hand, the ESP of CB $n$  reveals the negatively charged carbonyl regions (in red) and the electron-deficient equatorial region (in blue), which offer docking points for the cluster dianions through ion–dipole interactions. Scrutiny of the literature reveals that the tendency of some anions to associate with the outer walls of CB $n$  macrocycles has already been documented,<sup>13</sup> but not appreciated as a generic recognition motif, operative selectively for chaotropic anions. For example, Tao and coworkers have shown that coordination polymers based on CB $n$  can be achieved in the presence of inorganic anions

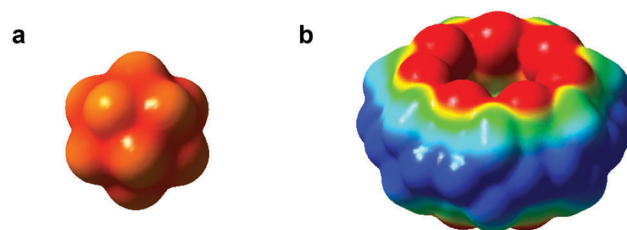


Fig. 4 DFT computed electrostatic potential maps for  $\text{B}_{12}\text{H}_{12}^{2-}$  and CB7. Electron-rich and -deficient regions shown in red and blue, respectively.



(e.g.,  $\text{ZnCl}_2^{2-}$ ,  $\text{PtCl}_6^{2-}$ , and  $\text{CdCl}_4^{2-}$ ).<sup>13a-e</sup> Fang *et al.* also reported that  $\text{CB}_n$  and polyoxometalates form hybrid organic-inorganic assemblies.<sup>13f</sup>

The symmetrical nature of both, dodecaborates and  $\text{CB}_n$ , allows the assembly motif to be expanded into three dimensions, into a supramolecular network. We presume therefore, in aqueous solution, that the chaotropic effect drives the borate cluster anions to the walls of the  $\text{CB}_n$  macrocycles where they dock according to the electrostatic potentials and ultimately form aggregates (Fig. 1). The large size of the borate cluster anions therefore allows multiple interactions to occur, which phenomenologically leads to a “salting-out effect” of an organic solute. This is against chemical intuition, because salting-out effects are otherwise characteristic for kosmotropic ions.

The  $\text{CB}_n$  aggregation induced by dodecaborate anions was observed at low millimolar concentrations ( $>0.1$  mM) of the clusters and  $\text{CB}_n$ . Fig. 5a and b show the SEM and TEM images of the formed aggregates. The multiple connectivity of the assemblies is in line with the dodecaborate clusters acting as bridges that link several  $\text{CB}_7$  units together. Similar aggregates were observed when  $\text{Na}_2\text{B}_{12}\text{Cl}_{12}$  was mixed with  $\text{CB}_7$  (Fig. S5, ESI†). Interestingly, the  $\text{CB}_7/\text{B}_{12}\text{H}_{12}^{2-}$  self-assembly can be reversibly controlled by changing the pH (Fig. 1). The aggregates can be partially disassembled by concentrated acid (Fig. S6a and b, ESI†) and re-generated upon dilution or pH-neutralization (Fig. S6c and d, ESI†). The partial disassembly of the aggregates in strongly acidic solution is attributed to a competitive binding of acid (hydronium ions) to the dodecaborate clusters.

In contrast to common chaotropic anions, borate clusters have the advantage that they can be easily functionalized and tethered to organic residues, an option based on which we expanded our study. In particular, this allowed us to assemble responsive supramolecular structures by exploiting the chaotropic and hydrophobic effects as orthogonal interactions. In detail, we have tethered dodecaborate to an azobenzene (AZO) moiety, which is known to be encapsulated by  $\text{CB}_7$  (hydrophobic effect under inclusion complex formation) and to undergo *trans-to-cis* photoisomerization (Fig. 1b).<sup>14</sup> The ditopic guest **G1** showed the ability

to self-assemble on its own, because the dodecaborate cluster has also an affinity to the AZO group (chaotropic effect). SEM and TEM images showed that **G1** formed spherical nanoparticles (Fig. 5c and d), while DLS measurement resulted in an average hydrodynamic diameter of 125 nm (Fig. S12, ESI†).

Multi-responsive assemblies were prepared by mixing **G1** and  $\text{CB}_7$  in aqueous solution. The hydrophobic effect drives the *trans*-azobenzene residue into the cavity of  $\text{CB}_7$ , while the chaotropic effect allows dodecaborate anions to dock to the exterior of  $\text{CB}_7$  according to the binding motif established above. Fig. 1b shows one possible cross-sectional view of various structures of the anticipated multi-responsive assembly, and its reversible changes as controlled by light and pH. The orthogonal self-assembled supramolecular networks grew with time (hours). Due to the self-aggregation of **G1** and the  $\text{CB}_7/\text{G1}$  assembly in water, NMR spectroscopy was unsuitable for further characterization. However, the  $^1\text{H}$  NMR spectra of 4-phenylazophenol in the presence of  $\text{CB}_7$  verified that the AZO residue in its *trans* configuration forms an inclusion complex with  $\text{CB}_7$  (Fig. S13, ESI†). Shear viscosity of the  $\text{CB}_7/\text{G1}$  complex increased steeply with a low shear rate and decreased gradually after that, and shear stress of the complex was higher than that of single components, which indicated the formation of the complex (Fig. S14, ESI†). The morphology of the  $\text{CB}_7/\text{G1}$  assembly was obtained by SEM and TEM (Fig. 5e and f). In comparison to the  $\text{CB}_7/\text{B}_{12}\text{H}_{12}^{2-}$  aggregates, the  $\text{CB}_7/\text{G1}$  aggregates are more compact, due to the additional inclusion complexation.

The propensity of the AZO moiety to undergo *trans-to-cis* photoisomerization in **G1** and the  $\text{CB}_7/\text{G1}$  assemblies was confirmed by UV-Vis spectra before and after 350 nm irradiation, see Fig. 6a, which provided evidence that both **G1** and  $\text{CB}_7/\text{G1}$  undergo *trans-to-cis* photoisomerization. As an additional independent line of evidence for the retained photoactivity, we have now

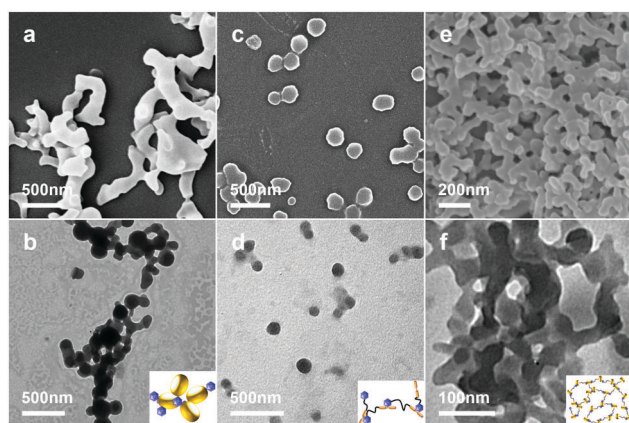


Fig. 5 (a) SEM and (b) TEM images of  $\text{CB}_7/\text{Na}_2\text{B}_{12}\text{H}_{12}$  aggregates. (c) SEM and (d) TEM images of **G1** in aqueous solution aged for 24 h. (e) SEM and (f) TEM images of the  $\text{CB}_7/\text{G1}$  assembly, aged for 24 h in aqueous solution.

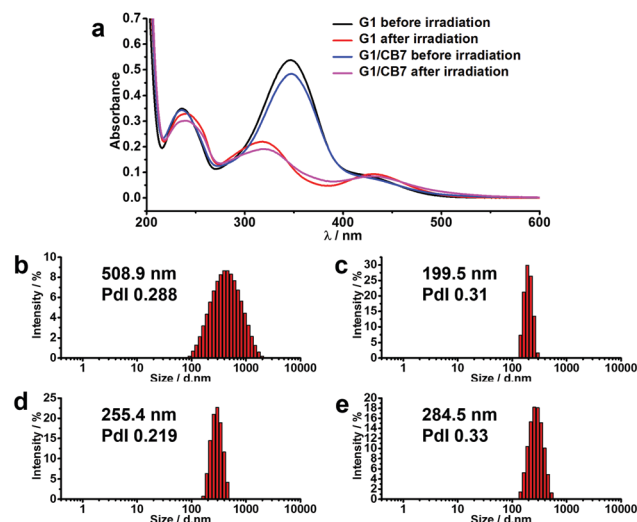


Fig. 6 (a) UV-Vis spectra of **G1** and  $\text{CB}_7/\text{G1}$  before and after UV irradiation in water ( $\lambda = 350$  nm). DLS results for the  $\text{CB}_7/\text{G1}$  complex (b) in aqueous solution, (c) in aqueous solution and irradiation with UV light for 30 min, (d and e) upon exposing to visible light for 100 s and 200 s after irradiation with UV light for 30 min, respectively.



also prepared a highly water-soluble model compound (G2, ESI<sup>†</sup>). The photoisomerization was also observed by <sup>1</sup>H NMR spectroscopy (ESI,† Fig. S16), in which only the *trans* form of azobenzene could be encapsulated in the cavity of CB7. Although both isomers are hydrophobic, only the elongated *trans* form displays a good shape fitting and adapted electronic properties to allow an axial threading through both CB7 portals.<sup>14a</sup>

The size measured by DLS of the CB7/G1 aggregate showed an average hydrodynamic diameter of 500 nm (Fig. 6b), which decreased to 200 nm upon irradiation for 30 minutes (Fig. 6c). Moreover, SEM and TEM images showed that, after irradiation by UV light, the former networks transformed into spherical nanoparticles, hinting to the anticipated change in the structure of the assemblies (see ESI,† Fig. S17a and b). When the disassembled system was exposed to visible light, the average hydrodynamic diameter of the system increased with irradiation time (Fig. 6d and e). Furthermore, when the system was heated to 60 °C, larger aggregates were formed (Fig. S19, ESI<sup>†</sup>).

As the exclusion complexes of dodecaborate clusters with CB7 can be partially disassembled at low pH values in a reversible manner, a multi-responsive material is obtained. The SEM and TEM images of CB7/G1 dissolved in formic acid (88%) showed the disassembly of the aggregate and transformation into spherical nanoparticles with 300–500 nm size (see ESI,† Fig. S17c and d). The addition of acid to the CB7/G1 system breaks down the CB7/dodecaborate exclusion complexation (partially “neutralizes” the chaotropic effect), while irradiation by UV light leads to the dissociation of the inclusion complexation between the AZO-residue and CB7 (“neutralizes” the hydrophobic effect). The nanoparticles formed in formic acid solution displayed a different size compared to those formed upon irradiation. ESI-MS conducted in formic acid (88%) indicated a 1 : 1 complexation of G1 with CB7, providing evidence for the existence of non-aggregated, stoichiometric complexes (Fig. S20 (ESI<sup>†</sup>), *m/z* 1521.20). When the partially disassembled system was aged for a month with evaporation of the acid, the networks reassembled (Fig. S21, ESI<sup>†</sup>).

In summary, new assemblies between dodecaborate anions and CB $n$  have been reported, which exploit the chaotropic effect in the context of functional materials. In the assemblies, dodecaborate anions formed exclusion complexes with CB7 driven by the chaotropic effect, leaving the cavity accessible to bind other organic guest molecules by the hydrophobic effect. Novel multi-responsive dodecaborate-cucurbituril supramolecular networks were developed based on orthogonal hydrophobic-chaotropic interactions allowing exclusion and inclusion complexation. The multi-responsive assemblies were conveniently assembled in aqueous solution at ambient temperature, establishing a new platform to prepare supramolecular polymer networks under mild conditions.

This work was financially supported by the Fundamental Research Funds for the Central Universities (no. 2042016HF1054) and Wuhan University Experiment Technology Project Funding

(no. WHU-2016-SYJS-06). We are grateful to Prof. Dr Dongsheng Guo (Nankai University) for fruitful discussion. And we are grateful to Dr Wenjing Liu (Nanjing Normal University) and Dr Zhengguo Lin (Beijing Institute of Technology) for assistance of crystallography. K. I. A. and W. M. N. are grateful to the DFG for the support within grant NA-686/8. The work was initiated through a fellowship of the China Scholarship Council (no. 201406275086) supporting the research of H. Z. at Jacobs University Bremen.

## Conflicts of interest

There are no conflicts to declare.

## Notes and references

- (a) B. Moulton and M. J. Zaworotko, *Chem. Rev.*, 2001, **101**, 1629; (b) L. Brunsveld and E. W. Meijer, *Chem. Rev.*, 2001, **101**, 4071; (c) L. Voorhaar and R. Hoogenboom, *Chem. Soc. Rev.*, 2016, **45**, 4013; (d) C. Heinzmann, C. Weder and L. Montero de Espinosa, *Chem. Soc. Rev.*, 2016, **45**, 342.
- (a) Q.-D. Hu, G.-P. Tang and P. K. Chu, *Acc. Chem. Res.*, 2014, **47**, 2017; (b) A. Alsaiee, D. E. Helbling and W. R. Dichtel, *Nature*, 2016, **529**, 190; (c) S. Zhang, *Nat. Biotechnol.*, 2003, **21**, 1171; (d) S. I. Stupp, *Science*, 1997, **276**, 384.
- (a) X. Dai and W. Liu, *Adv. Mater.*, 2015, **27**, 3566; (b) F. Luo and J. P. Gong, *Adv. Mater.*, 2015, **27**, 2722; (c) L. R. Hart, H. M. Colquhoun and W. Hayes, *Polym. Chem.*, 2014, **5**, 3680; (d) E. A. P. Appel and M. W. Tibbitt, *Nat. Commun.*, 2015, **6**, 6295; (e) A. P. Constantinou and T. K. Georgiou, *Polym. Chem.*, 2016, **7**, 2045; (f) A. Noro and Y. Matsushita, *Macromolecules*, 2013, **46**, 8304.
- (a) X. Yan, F. Huang and P. J. Stang, *J. Am. Chem. Soc.*, 2014, **136**, 4460; (b) H. Chen, X. Ma and H. Tian, *Angew. Chem., Int. Ed.*, 2014, **53**, 14149; (c) Q. Yan and J. Yuan, *Polym. Chem.*, 2013, **4**, 1216; (d) S. Dong and F. Huang, *Acc. Chem. Res.*, 2014, **47**, 1982; (e) N. Song and Y.-W. Yang, *Chem. Commun.*, 2014, **50**, 8231.
- (a) C. Douvris and J. Michl, *Chem. Rev.*, 2013, **113**, PR179; (b) K. Karki and D. Roccatano, *Inorg. Chem.*, 2012, **51**, 4894.
- (a) J. Plešek, *Chem. Rev.*, 1992, **92**, 269; (b) W. Tjarks, *Chem. Commun.*, 2007, 4978.
- (a) K. I. Assaf, K. Rissanen, D. Gabel and W. M. Nau, *Angew. Chem., Int. Ed.*, 2015, **54**, 6852; (b) K. I. Assaf and W. M. Nau, *Org. Biomol. Chem.*, 2016, **14**, 7702; (c) K. I. Assaf, *Org. Lett.*, 2016, **18**, 932.
- R. Fernandez-Alvarez and Pavel Matějček, *Langmuir*, 2017, DOI: 10.1021/acs.langmuir.7b03306.
- F. Biedermann, W. M. Nau and H.-J. Schneider, *Angew. Chem., Int. Ed.*, 2014, **53**, 11158.
- (a) W. A. Freeman and W. L. Mock, *J. Am. Chem. Soc.*, 1981, **103**, 7367; (b) J. Kim and K. Kim, *J. Am. Chem. Soc.*, 2000, **122**, 540; (c) J. Lagona and L. Isaacs, *Angew. Chem., Int. Ed.*, 2005, **44**, 4844; (d) K. I. Assaf and W. M. Nau, *Chem. Soc. Rev.*, 2015, **44**, 394.
- (a) M. Florea and W. M. Nau, *Angew. Chem., Int. Ed.*, 2011, **50**, 9338; (b) S. J. Barrow and O. A. Scherman, *Chem. Rev.*, 2015, **115**, 12320; (c) D. Shetty and K. Kim, *Chem. Soc. Rev.*, 2015, **44**, 8747.
- (a) E. A. Appel and O. A. Scherman, *J. Am. Chem. Soc.*, 2010, **132**, 14251; (b) L. Chen and X. Zhang, *Polym. Chem.*, 2016, **7**, 1397.
- (a) H. Cong, K. Chen and Z. Tao, *Eur. J. Inorg. Chem.*, 2014, 2262; (b) N.-N. Ji and Z. Tao, *Eur. J. Inorg. Chem.*, 2014, 1435; (c) Y. Zhao, L.-L. Liang and Q.-J. Zhu, *CrystEngComm*, 2013, **15**, 7987; (d) L.-L. Liang, Z. Tao and J.-X. Liu, *CrystEngComm*, 2013, **15**, 3943; (e) L. L. Liang, X. L. Ni and Z. Tao, *Inorg. Chem.*, 2013, **52**, 1909; (f) X. Fang and P. Kögerler, *J. Am. Chem. Soc.*, 2009, **131**, 432; (g) T. Goel, A. C. Bhasikuttan and J. Mohanty, *Chem. Commun.*, 2016, **52**, 7306.
- (a) M. Baroncini and S. Silvi, *Chem. – Eur. J.*, 2014, **20**, 10737; (b) J. Wu and L. Isaacs, *Chem. – Eur. J.*, 2009, **15**, 11675; (c) S. Choi and K. Kim, *Chem. Commun.*, 2003, 2176.

